A warm-season comparison of WRF coupled to the CLM4.0, Noah-MP, and Bucket hydrology land surface schemes over the central USA

Matthew S. Van Den Broeke
University of Nebraska-Lincoln, mvandenbroeke2@unl.edu

Andrew Kalin
NOAA/National Weather Service

Jose Abraham Torres Alavez
University of Nebraska-Lincoln

Robert Oglesby
University of Nebraska-Lincoln & Daugherty Water for Food Institute

Q. Steven Hu
University of Nebraska - Lincoln, qhu2@unl.edu

Theor Appl Climatol (2018) 134:801–816
https://doi.org/10.1007/s00704-017-2301-8

ORIGINAL PAPER

A warm-season comparison of WRF coupled to the CLM4.0, Noah-MP, and Bucket hydrology land surface schemes over the central USA

Matthew S. Van Den Broeke[1] · **Andrew Kalin**[2] · **Jose Abraham Torres Alavez**[1] · **Robert Oglesby**[1,3,4] · **Qi Hu**[3,1]

Received: 26 January 2017 / Accepted: 9 October 2017 / Published online: 4 November 2017

Abstract In climate modeling studies, there is a need to choose a suitable land surface model (LSM) while adhering to available resources. In this study, the viability of three LSM options (Community Land Model version 4.0 [CLM4.0], Noah-MP, and the five-layer thermal diffusion [Bucket] scheme) in the Weather Research and Forecasting model version 3.6 (WRF3.6) was examined for the warm season in a domain centered on the central USA. Model output was compared to Parameter-elevation Relationships on Independent Slopes Model (PRISM) data, a gridded observational dataset including mean monthly temperature and total monthly precipitation. Model output temperature, precipitation, latent heat (LH) flux, sensible heat (SH) flux, and soil water content (SWC) were compared to observations from sites in the Central and Southern Great Plains region. An overall warm bias was found in CLM4.0 and Noah-MP, with a cool bias of larger magnitude in the Bucket model. These three LSMs produced similar patterns of wet and dry biases. Model output of SWC and LH/SH fluxes were compared to observations, and did not show a consistent bias. Both sophisticated LSMs appear to be viable options for simulating the effects of land use change in the central USA.

✉ Matthew S. Van Den Broeke
mvandenbroeke2@unl.edu

[1] Department of Earth and Atmospheric Sciences, University of Nebraska-Lincoln, 306 Bessey Hall, Lincoln, NE 68588-0340, USA

[2] NOAA/National Weather Service, Spokane, WA, USA

[3] School of Natural Resources, University of Nebraska-Lincoln, Lincoln, NE, USA

[4] Daugherty Water for Food Institute, Lincoln, NE, USA

1 Introduction

The state of the land use/land cover (LULC) is a critical component of the regional climate system via interactions between the land surface and the overlying atmosphere. LULC directly affects land surface albedo, altering the local surface energy balance (e.g., Charney et al. 1975; Otterman et al. 1984; Giambelluca et al. 1997). Different LULC conditions are also associated with varying leaf area indexes (LAIs), which influence the partitioning of absorbed solar radiation between latent and sensible heat flux from the surface (Copeland et al. 1996). The ratio of sensible to latent heat flux, known as the Bowen ratio (Bowen 1926), strongly influences the moisture and temperature characteristics of the overlying atmosphere and regional and large-scale atmospheric circulations. A larger LAI is associated with a stronger vegetation influence on surface albedo and Bowen ratio.

By affecting surface evaporation, LULC also influences soil moisture and the local water budget (e.g., Oglesby and Erickson 1989; Oglesby et al. 2001). Different vegetation conditions are associated with different rooting depths, which influence the ability for plants to draw on deep soil moisture, and evapotranspiration (ET) rates (Oglesby et al. 2002). The state of LULC can also influence variables related to the regional- and larger-scale circulation. For example, land cover changes in western Australia have been related to changes in the depth of the planetary boundary layer (PBL) and placement of the west coast trough. Convective clouds and precipitation are more common over diverse native vegetation than over the more uniform vegetation of an agricultural region (Lyons et al. 1993; Nair et al. 2011). Large differences in energy fluxes between land cover types may also result in the development of mesoscale circulations (e.g., Pielke et al. 1991; Weaver 2004), which may then result in favored areas for precipitation development (e.g., Anthes 1984). Irrigation is another example of an anthropogenic land surface modification which may result in changes to the regional circulation and precipitation patterns. In the central USA, irrigation associated with agriculture has increased local soil water content (SWC) and decreased soil temperature relative to what would occur in the absence of irrigation (e.g., Mahmood et al. 2006, 2008). In many regions, irrigation has been observed to increase regional precipitation and decrease temperature (e.g., as reviewed by Mahmood et al. 2014). Irrigation and crop growth should be considered together to achieve optimal model results (e.g., Lu et al. 2015). In the Great Plains region, which was the focus of this study, irrigation has been found to potentially influence the structure of the low-level jet and to result in a substantial increase in downstream precipitation (Huber et al. 2014).

When describing the influence of LULC on regional climate, a land surface model (LSM) is necessary to represent high-resolution variations in vegetation, surface, and subsurface properties. LSMs may be used to simulate hydrologic, biogeophysical, and biogeochemical processes involved in land surface-atmosphere interactions (e.g., Wei et al. 2010). A variety of LSMs are available, which differ in level of complexity and physical parameterizations (e.g., Pitman 2003), in the computational expense to run, and in the output variables provided. Thus, when selecting a LSM for a particular study, the nature of the proposed study should be a key consideration in order to ensure the strengths of the LSM align appropriately with the study's research objectives (Luo et al. 2012). Different LSMs may perform better or worse in particular geographic regions. Given these factors, metrics and statistical measures across several variables and scales should be used to assess model performance prior to selecting an LSM for particular study goals. These measures should be drawn from key traceable components such as precipitation, temperature, and surface fluxes.

In our domain of interest, a summertime warm temperature bias has been noted in prior 4-km WRF simulations (Liu et al. 2016). Their simulations were characterized by the largest warm bias in the central USA during the warm season (e.g., Fig. 12 of Liu et al. 2016). Liu et al. speculate that the warm bias may result from lack of cloud cover and/or from a feedback loop in which low soil moisture anomalies result in anomalously low regional precipitation. They also noted that the central USA warm bias was most pronounced in dry years. A similar warm bias has been found over portions of East Asia (Fig. 5 of Li et al. 2016). This warm bias was related to a larger sensible heat flux over land, especially in dry areas, and resulted in a larger land-sea temperature difference. This in turn led to stronger moisture transport and overestimated precipitation in the monsoon region of southern China (Li et al. 2016).

The purpose of this study is to evaluate the ability of two sophisticated LSMs, the Community Land Model version 4.0 (CLM4.0) and Noah-MP, along with one simple reference LSM, the Budyko Bucket Hydrology model (henceforth referred to as "Bucket model" or "Bucket option"), to realistically simulate warm-season temperature, precipitation, and surface energy fluxes in high-resolution simulations over the central USA. This region and season is our focus since there is a lack of LSM comparisons in the literature for any season in this region. This study helps address this need by determining each LSM's biases in this domain during the warm season. This region is also known for large interannual precipitation variability and summertime drought susceptibility (e.g., Woodhouse and Overpeck 1998; Mo and Schemm 2008), making the choice of an appropriate LSM particularly important for warm-season regional simulations. Examining LSM performance here is critical for future studies, especially those examining the effects of LULC on precipitation and the regional atmospheric circulation.

2 Methods

The Weather Research and Forecasting model v. 3.6 (WRF3.6; Skamarock et al. 2008) was used in this study, coupled to three different LSMs: CLM4.0, Noah-MP, and the Bucket model. Each LSM differs in degree of complexity and ability to estimate surface fluxes. A nested domain was used, with an outer domain covering the USA and surrounding waters at 12 km resolution and an inner domain in the central USA at 4 km resolution (approximately 28°–43° N and 94°–106° W; Fig. 1). Lateral boundary conditions were provided by the North American Regional Reanalysis (NARR) dataset (Mesinger et al. 2006) at 32-km horizontal resolution. One caveat about use of NARR data is that its highest vertical level is 100 hPa, resulting in possible influence to simulated circulations and deep convection. A high-resolution inner domain was used since prior studies have indicated that model results (e.g., temperature and precipitation output) are likely to improve with higher horizontal resolution (e.g., Hack et al. 2006; Rojas 2006). It is unclear, however, how much improvement might be expected by increasing the model resolution from 12 to 4 km. Rojas (2006) found relatively small improvements when model resolution was decreased from 45 to 15 km, and Hack et al. (2006) showed no clear improvement with increased model resolution for some atmospheric and oceanic variables.

Land use categorization in WRF3.6 was determined from the default United States Geological Survey (USGS) 24 land use categories. Simulations were run for 2006, 2007, and 2012, representing climatologically normal, wet, and dry years, respectively, over much of the inner domain. They started on January 1 of each year and ran for the entire year. Results for the months of April, June, and August from each of these 3 years were chosen for analysis to examine differences in LSMs in describing interactions between large-scale

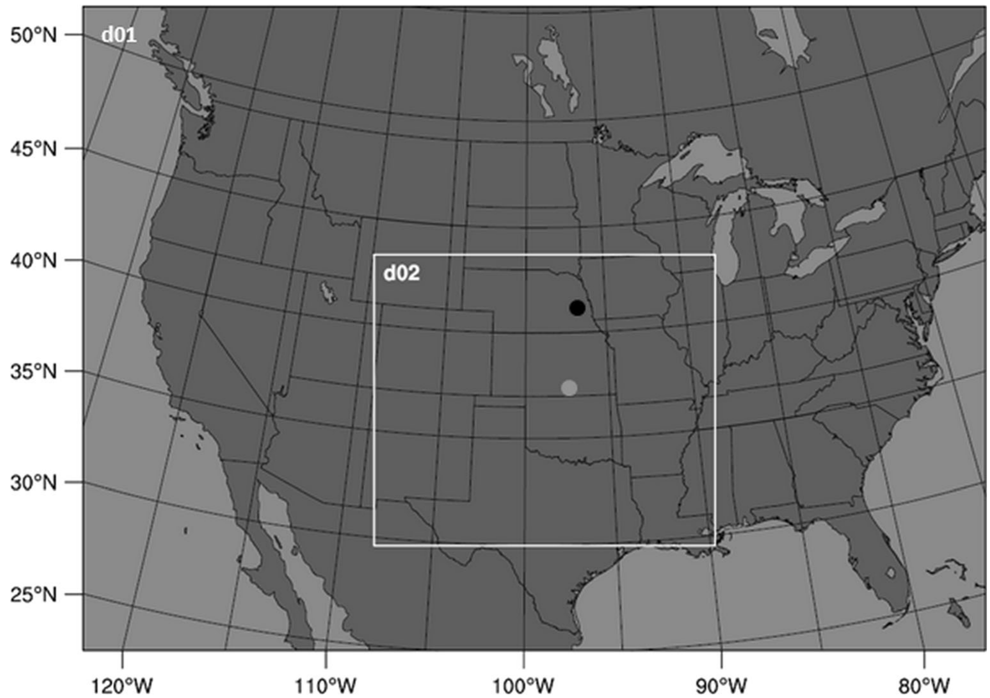

Fig. 1 Inner (4 km; d02) and outer (12 km; d01) domains of WRF simulations. Locations of the Mead, Nebraska, AmeriFlux site (black dot) and the Ashton, Kansas, ARM site (gray dot) are indicated

forcing and land surface processes during the growing season. These months were chosen to represent the early, middle, and late growing seasons in the US Great Plains.

The WRF Single-Moment 5-class scheme (Hong et al. 2004) was used for cloud microphysics, the Kain-Fritsch scheme (Kain and Fritsch 1990; Kain 2004) for cumulus parameterization (as in, e.g., Bukovsky and Karoly 2009), and the Dudhia (1989) and rapid radiative transfer model (RRTM; Mlawer et al. 1997) schemes for shortwave and longwave radiation, respectively. These parameterization choices appear to simulate reasonably well the appropriate atmospheric processes across the model domain. The Kain-Fritsch cumulus parameterization was used for both inner and outer domains. A potential approach in future simulations, given the 4-km resolution on the inner domain, would be to test a convection-permitting scheme if computationally possible (e.g., Prein et al. 2015).

2.1 CLM4.0 and Noah-MP

The CLM4.0 consists of five primary sub-grid land cover types including glacier, lake, wetland, urban, and vegetation, with vegetation being subdivided into seven primary plant functional types. Each type is associated with a representative leaf and stem area index and canopy height (Oleson et al. 2010; Lawrence et al. 2011). CLM4.0 allows multiple vegetation types per grid cell to improve flux estimations. A total of 24 land cover types are available in CLM4.0. Temperature is calculated for 15 subsurface layers, partitioned into 10 soil layers unevenly spaced between the top layer (0.0–0.018 m) and the bottom layer (2.296–3.802 m), and 5 bedrock layers to a depth of 42 m. Soil temperature and moisture are calculated for each soil layer. Enhancements and improvements in CLM4.0 compared to the previous version of CLM include cooler temperature in high-organic soils, reduced albedo over forest and grassland, more robust soil moisture estimates, and greater areal snow coverage (Lawrence et al. 2011). The default static vegetation was used for this study since dynamic vegetation models, which allow for changes in LAI through the year, are yet to be fully tested.

Previous investigations (e.g., Lu and Kueppers 2012) showed that WRF v. 3 coupled with the earlier CLM v. 3.5 (WRF3-CLM3.5) tended to overestimate wintertime precipitation and underestimate summer precipitation when compared to observations from AmeriFlux sites. Additionally, both WRF3-CLM3.5 and WRF3 coupled to the Noah LSM (WRF3-Noah) tended to overestimate downward solar radiation, for which an underestimate of cloud cover may be responsible (Lu and Kueppers 2012). WRF3-CLM3.5 and WRF3-Noah both overestimated sensible heating and thus produced a warm bias in 2-m temperature. When considering the western USA, WRF3-CLM3.5 did best in overall comparison to the soil thermal diffusivity (STD), Rapid Update Cycle (RUC), and Noah land surface schemes (Jin et al. 2010). CLM3.5, Noah-MP, and especially Noah coupled with WRF3.5 produced a cold bias at the surface in winter in the western USA, likely due to overestimating albedo (Chen et al. 2014). All three LSMs overestimated precipitation compared to Snow Telemetry (SNOTEL) sites, though gauge accuracy of the SNOTEL sites may have influenced the results (Chen

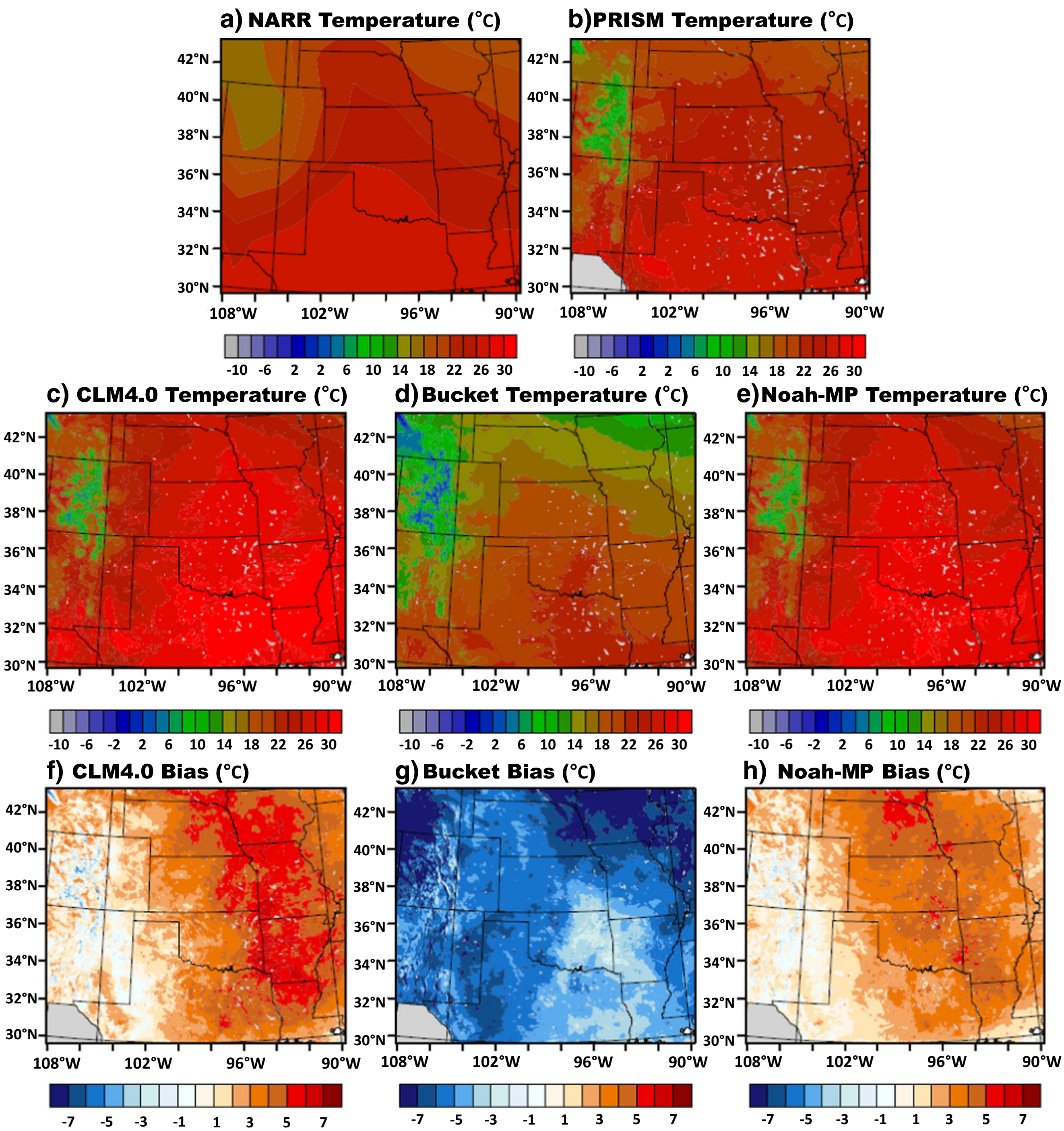

Fig. 2 Spatial temperature distribution (°C) for June 2006 over the inner domain. **a** NARR. **b** PRISM. **c–e** Model output from CLM4.0, Bucket, and Noah-MP. **f–h** Model bias (model minus PRISM). The white dots located throughout many of the plots coincide with bodies of water

et al. 2014). When comparing WRF3-Noah and WRF3-CLM3.5 in California, both captured the broad spatial and seasonal temperature patterns while overestimating daily minimum temperature, with WRF-Noah having the larger bias (Subin et al. 2011). WRF3-CLM3.5 also performed better with dewpoint values, but was drier than observations. Both WRF3-Noah and WRF3-CLM3.5 suffer from a high precipitation bias.

Noah-MP parameterizes various land, atmosphere, and hydrologic processes (Niu et al. 2011). It contains four soil layers, up to three snow layers, and one canopy layer, with a sub-grid scheme to allow for gaps in the vegetation canopy.

Table 1 Mean monthly 2-m temperature (°C), and bias, root mean square error (RMSE), standard deviation (SD), and spatial correlation coefficient (*r*) compared to PRISM data over the inner domain (4 km horizontal resolution) for April, June, and August of 2006, 2007, and 2012

2-m air temperature (°C)															
2006															
	April					June					August				
	Mean	Bias	RMSE	SD	r	Mean	Bias	RMSE	SD	r	Mean	Bias	RMSE	SD	*r*
PRISM	15.1	–	–	4.9	–	23.3	–	–	3.4	–	24.7	–	–	4.2	–
NARR	16.1	+ 1.0	1.6	5.3	0.97	24.9	+ 1.6	1.9	3.7	0.96	26.2	+ 1.5	1.8	4.3	0.97
CLM4.0	16.4	+ 1.3	1.8	5.3	0.97	26.4	+ 3.1	3.7	4.3	0.90	27.1	+ 2.4	3.1	5.2	0.95
Noah-MP	16.2	+ 1.1	1.7	5.3	0.97	25.9	+ 2.6	3.1	4.0	0.93	26.5	+ 1.8	2.4	4.8	0.96
Bucket	12.0	− 3.1	3.4	4.8	0.97	17.7	− 5.6	5.8	4.1	0.95	18.1	− 6.6	6.9	4.2	0.90
2007															
	April					June					August				
	Mean	Bias		SD		Mean	Bias		SD		Mean	Bias		SD	
PRISM	11.0	–		4.1		22.2	–		3.5		25.5	–		3.5	
NARR	12.1	+ 1.1		4.4		23.6	+ 1.4		3.5		26.7	+ 1.2		3.4	
CLM4.0	11.3	+ 0.3		4.4		24.1	+ 1.9		4.0		28.8	+ 3.3		4.9	
Noah-MP	11.4	+ 0.4		4.5		23.4	+ 1.2		4.0		28.2	+ 2.7		4.7	
Bucket	8.6	− 2.4		5.4		16.5	− 5.7		4.5		17.2	− 8.3		4.3	
2012															
	April					June					August				
	Mean	Bias	RMSE	SD	*r*	Mean	Bias	RMSE	SD	*r*	Mean	Bias	RMSE	SD	*r*
PRISM	14.8	–	–	4.6	–	24.0	–	–	3.3	–	24.6	–	–	3.5	–
NARR	16.1	+ 1.3	1.6	4.7	0.97	25.3	+ 1.3	1.7	3.5	0.95	26.2	+ 1.6	1.9	3.3	0.95
CLM4.0	15.8	+ 1.0	1.5	5.2	0.98	27.6	+ 3.6	4.0	4.3	0.91	27.9	+ 3.3	3.8	4.2	0.91
Noah-MP	15.8	+ 1.0	1.5	5.1	0.98	26.6	+ 2.6	3.0	4.2	0.93	27.1	+ 2.5	2.9	3.8	0.94
Bucket	12.3	− 2.5	2.8	5.2	0.98	18.4	− 5.6	5.8	4.2	0.96	17.7	− 6.9	7.0	3.9	0.94

Noah-MP also contains a two-stream radiation transfer scheme to allow for consideration of a three-dimensional canopy structure, and utilizes a Ball-Berry photosynthesis-based stomatal resistance. It is capable of differentiating C3 and C4 photosynthesis pathways. Noah-MP provides enhancements from the less advanced Noah LSM, also an option in WRF, in vegetation canopy energy balance, layered snowpack, frozen soil and infiltration, and soil moisture-groundwater interaction (Niu et al. 2011). Default static vegetation was again imposed in the Noah-MP simulations.

2.2 Bucket model

A simple reference LSM, the five-layer thermal diffusion scheme (Dudhia 1996), here known as the Bucket model (e.g., Budyko 1961; Manabe 1969) or Bucket option, treats the land surface and underlying soil as a bucket that is filled by precipitation and snowmelt and emptied by evaporation. If the soil water level reaches a critical threshold (100% of field capacity), then the extra water in the "bucket" overflows as runoff. Evaporation rate varies linearly between zero and the potential evaporation rate based on the water level in the bucket. Sub-grid features are not allowed as in CLM4.0 and Noah-MP.

2.3 PRISM

To evaluate and validate the capability of WRF3.6 coupled with each of these LSMs, we compared the model output to data from the Parameter-elevation Relationships on Independent Slopes Model (PRISM), a gridded observational dataset which utilizes > 10,000 surface stations for temperature and nearly 13,000 stations for precipitation (Daly et al. 2008; PRISM Climate Group 2015). PRISM data represent the official US climate dataset for the Department of Agriculture, and account for several factors including elevation, topography, and coastal proximity to create a climate-elevation regression for each grid cell. The dataset provides values for, e.g., monthly and annual minimum, maximum, and mean temperature and total precipitation. PRISM data are available at 4-km resolution, and are re-gridded to a common

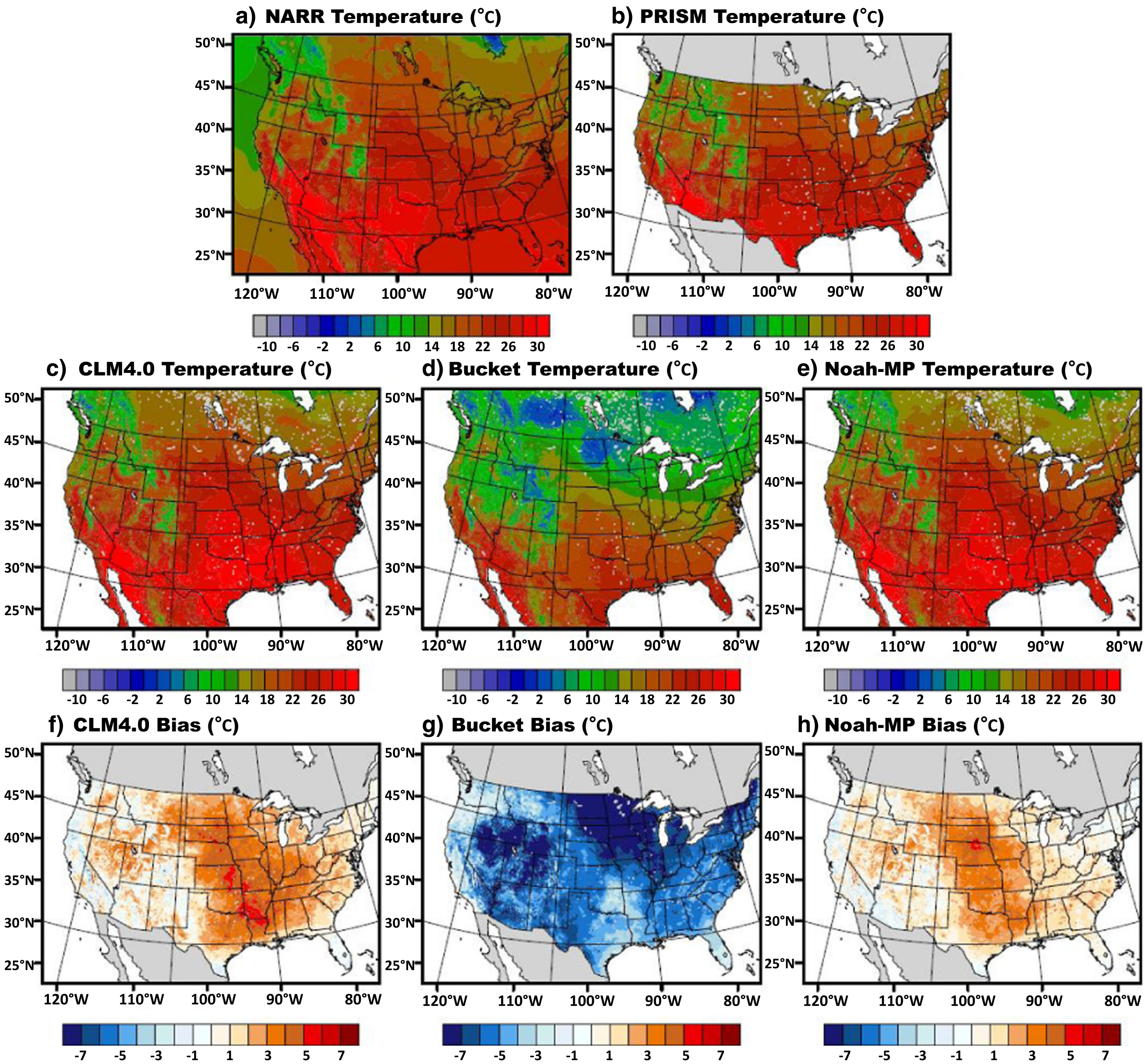

Fig. 3 Spatial temperature distribution (°C) for June 2006 over the outer domain. **a** NARR. **b** PRISM. **c**–**e** Model output from CLM4.0, Bucket, and Noah-MP. **f**–**h** Model bias (model minus PRISM). The white dots located throughout many of the plots coincide with bodies of water

grid for both the outer 12-km and inner 4-km domains of this study using bilinear interpolation.

2.4 ARM and AmeriFlux observations

Output from the inner domain of our simulations was compared to observed daily and seasonal variations in surface heat fluxes, SWC, precipitation, and temperature measured at sites from the Atmospheric Radiation Measurement (ARM) and AmeriFlux experiments. ARM is a network of highly instrumented ground stations operated by the US Department of Energy (DOE) originally developed to study cloud formation processes and their influence on radiative transfer (Huang and Liu 2015). The Southern Great Plains (SGP) facility consists of numerous sites centered near Lamont, Oklahoma. Of these, the site at Ashton, Kansas, was used in this study (Fig. 1). AmeriFlux is a global network of sites designed to measure CO_2, water, and energy fluxes (Baldocchi et al. 2001). Data from the AmeriFlux site at Mead, Nebraska (Fig. 1) were used in comparison with model outputs.

3 Results

Assessment of the model-simulated large-scale pattern was achieved by comparing mean monthly temperature and total

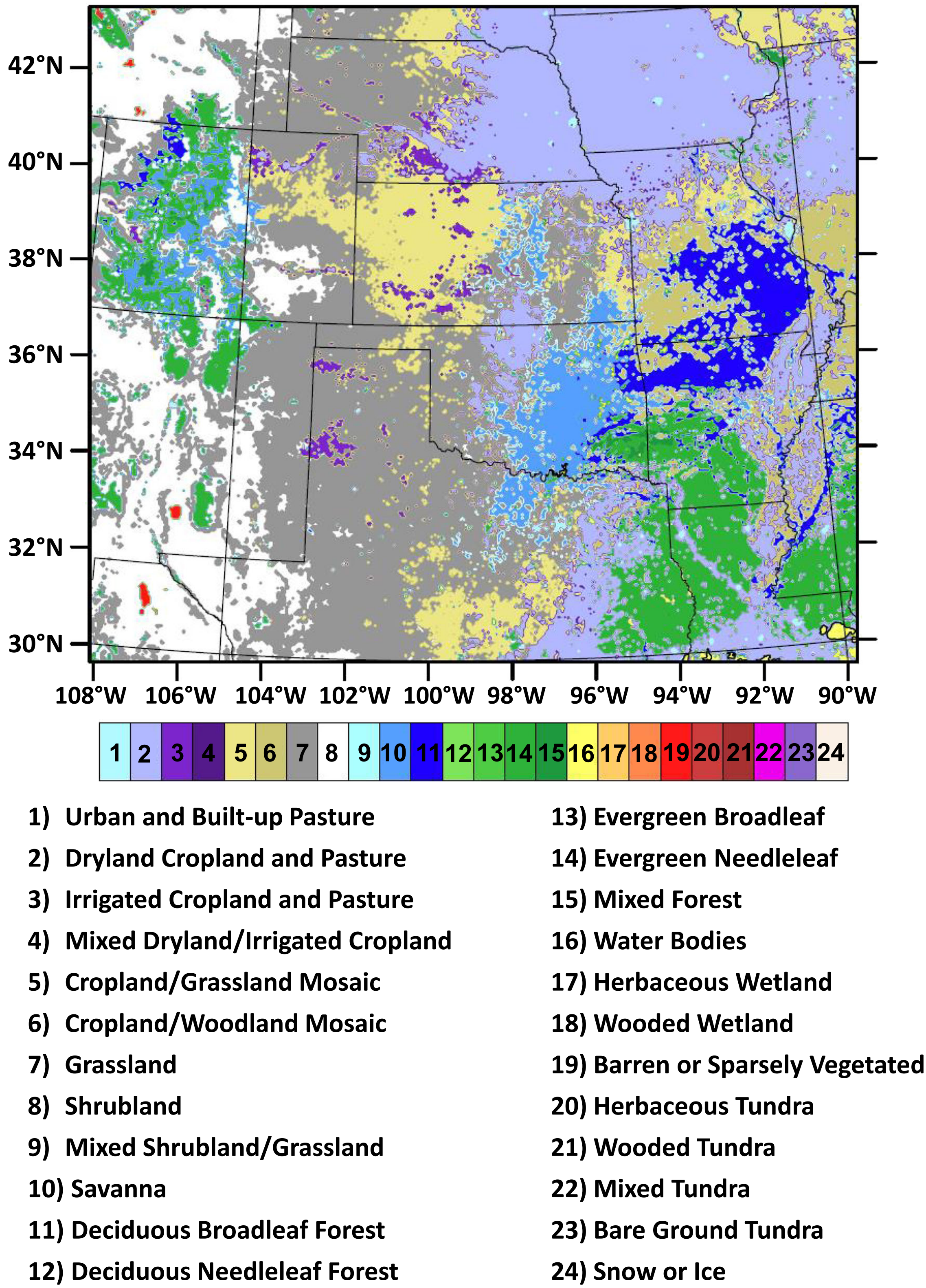

Fig. 4 Default land use (USGS 24 land use categories) in WRF3.6. Savanna (land cover classification 10) is a blue color primarily over eastern Oklahoma and adjacent areas

monthly precipitation from each WRF3.6/LSM combination with PRISM, NARR, and AmeriFlux data in the inner domain. Temperature and precipitation were chosen for comparison since they have the broadest and most complete

Table 2 Mean monthly precipitation (cm), and bias, root mean square error (RMSE), standard deviation (SD), and spatial correlation coefficient (*r*) compared to PRISM data over the inner domain (4 km horizontal resolution) for April, June, and August of 2006, 2007, and 2012

Monthly mean precipitation (cm)															
2006															
	April					June					August				
	Mean	Bias	RMSE	SD	*r*	Mean	Bias	RMSE	SD	*r*	Mean	Bias	RMSE	SD	*r*
PRISM	5.96	–	–	4.42	–	52.7	–	–	31.2	–	91.8	–	–	44.6	–
NARR	5.95	− 0.01	0.10	4.43	0.97	55.0	+ 2.3	1.1	32.0	0.94	94.8	+ 3.0	2.1	44.2	0.88
CLM4.0	7.06	+ 1.10	0.60	5.36	0.27	36.7	− 16.0	4.4	26.2	–	77.3	− 14.5	8.7	86.6	0.2
Noah-MP	6.46	+ 0.50	0.72	5.23	0.30	32.1	− 20.6	6.0	22.8	0.09	98.0	+ 6.2	9.9	81.0	0.07
Bucket	8.51	+ 2.55	0.70	6.66	0.39	63.4	+ 10.7	4.8	43.4	0.26	75.7	− 16.1	6.3	60.6	0.36
2007															
		April					June					August			
	Mean	Bias		SD		Mean	Bias		SD		Mean	Bias		SD	
PRISM	6.97	–		3.53		99.2	–		81.4		79.0	–		65.5	
NARR	6.53	− 0.44		3.38		89.5	− 9.7		71.5		80.6	+ 1.6		59.2	
CLM4.0	9.45	+ 2.48		5.29		81.8	− 17.4		55.9		35.7	− 43.3		47.9	
Noah-MP	8.44	+ 1.47		5.02		112.3	+ 13.1		110.7		46.1	− 32.9		52.4	
Bucket	9.84	+ 2.87		5.07		68.9	− 30.3		59.6		27.7	− 51.3		29.3	
2012															
		April					June					August			
	Mean	Bias	RMSE	SD	*r*	Mean	Bias	RMSE	SD	*r*	Mean	Bias	RMSE	SD	*r*
PRISM	5.83	–	–	4.07	–	43.5	–	–	33.9	–	59.5	–	–	59.8	–
NARR	6.39	+ 0.56	0.17	4.29	0.93	48.8	+ 5.3	1.8	34.4	0.89	66.7	+ 6.2	2.4	53.7	0.94
CLM4.0	6.27	+ 0.44	0.51	4.94	0.42	33.8	− 9.7	4.7	34.5	0.25	61.1	+ 1.6	7.4	67.3	0.36
Noah-MP	5.44	− 0.39	0.74	4.55	0.42	36.5	− 7.0	6.0	40.8	0.3	66.4	+ 6.9	8.8	72.8	0.44
Bucket	8.80	+ 2.97	0.70	5.71	0.23	68.7	+ 25.2	5.5	52.5	0.43	38.7	− 20.8	5.0	51.3	0.73

observational records and are indicators of atmospheric circulation and moisture transport.

3.1 Temperature

Across the inner domain, CLM4.0 and Noah-MP generally showed a warm bias compared to PRISM data (Fig. 2; Table 1), similar to the result obtained by Lu and Kueppers (2012) using WRF3-CLM3.5. Temperatures for June 2006 are shown in Fig. 2 as an example, since June is near the middle of the warm season and 2006 was a year with near-normal precipitation across the central USA. Conversely, when coupled to WRF3.6, the Bucket model results showed a cool bias (Fig. 2; Table 1), which was most prominent in the summer months. This may be because the Bucket model overestimates partitioning to latent heat, resulting in cooler temperatures than observed in dry situations. When the same comparison is made across the outer domain (Fig. 3), the same biases manifest there as well—CLM4.0 and Noah-MP have a slight warm bias across the eastern and western USA, though both exhibit a slight cool bias in high-elevation regions of the West. The Bucket model exhibits a larger-magnitude negative bias throughout the outer domain (Fig. 3), with a maximum bias approaching 10 °C in the northern Great Plains and western Great Lakes regions. In general, the highest-magnitude bias in CLM4.0 and Noah-MP is within the inner domain, while that in the Bucket model is north and west of the inner domain (Fig. 3). The pattern of bias in the sophisticated LSMs, however, does appear reasonably continuous across the boundary of the inner and outer domains, suggesting that increasing spatial resolution in the inner domain region may not meaningfully improve simulated temperature. This is generally consistent with prior studies (e.g., Rojas 2006). The magnitude of the warm bias was substantially higher (Table 1) in the normal year (2006) and dry year (2012) than in the wet year (2007), consistent with prior findings (e.g., Liu et al. 2016).

CLM4.0 and Noah-MP were also similar in their spatial patterns of overestimating 2-m air temperature, while the Bucket model produced a different spatial pattern (Fig. 2). It shows the largest cool bias in the north-central USA in April,

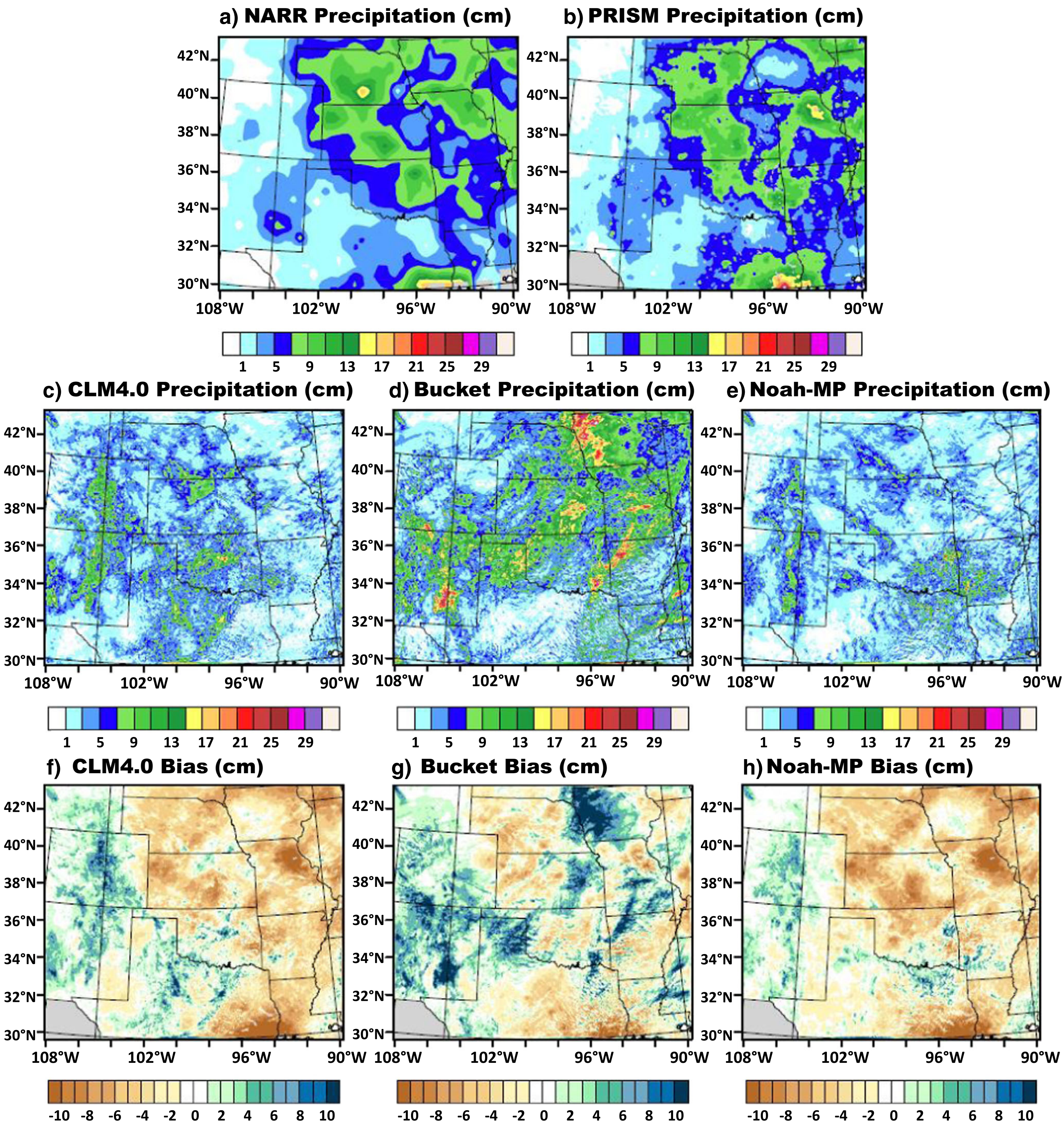

Fig. 5 Spatial precipitation distribution (cm) for June 2006 over the inner domain. **a** NARR. **b** PRISM. **c**–**e** Model output from CLM4.0, Bucket, and Noah-MP. **f**–**h** Model bias (model minus PRISM)

which spreads south through the growing season. A cool bias of smaller magnitude was present in June of all 3 years from north-central Texas through Oklahoma and into southeast Kansas (Fig. 2). This pattern continued through August (not shown), and was in relatively close alignment with savanna land cover (Fig. 4). By August, temperature bias over savanna was lower than over most other land cover types which account for a large percentage of this domain (Table 3). These results indicate that during this time period the Bucket model better represented SWC of a generic land surface type dominated by a combination of grasses and trees.

The magnitude of each LSM's temperature bias generally increased as the summer progressed in all three simulated years (Table 1). LSM performance was generally better over the first half of the growing season in 2007, which was a wet year in much of the inner domain, and

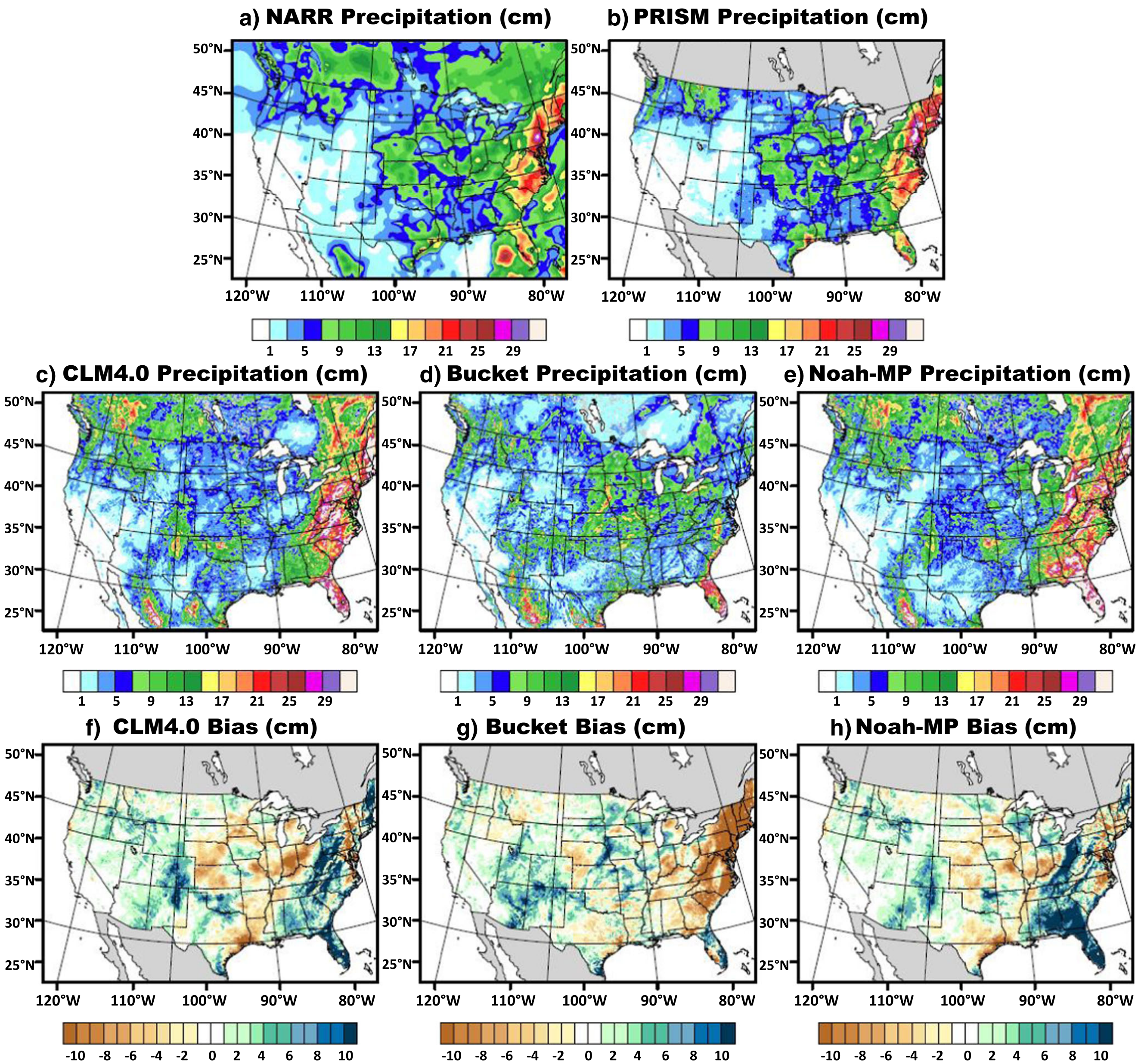

Fig. 6 Spatial precipitation distribution (cm) for June 2006 over the outer domain. **a** NARR. **b** PRISM. **c**–**e** Model output from CLM4.0, Bucket, and Noah-MP. **f**–**h** Model bias (model minus PRISM)

poorest in 2012, a regional drought year (Table 2). Poor performance during a drought year can partially be explained by the effect of agricultural practices, such as irrigation, on observed/PRISM values and the absence thereof in the simulations. Differences between the sophisticated LSMs (CLM4.0 and Noah-MP) and the Bucket model could also partially result from the fact that CLM4.0 and Noah-MP handle snowmelt and warming of the surface and subsurface layers more accurately. A warm bias in CLM4.0 and Noah-MP output may also be partially attributable to the fact that NARR data, which provided the boundary conditions for these simulations, were slightly warmer when compared to the PRISM dataset (Fig. 2a, b).

3.2 Precipitation

While Noah-MP and CLM4.0 produced generally similar precipitation patterns over the model inner domain, the Bucket model produced substantially more precipitation (Fig. 5; Table 2). This general similarity between CLM4.0 and Noah-MP and difference from the Bucket model is similar to the results for temperature. This is especially true in dry months and years, likely because

Table 3 Mean temperature bias (°C) over the inner domain for each LSM over several common central US land use categories

	April 2006			June 2006			August 2006		
	Bucket	Noah-MP	CLM4.0	Bucket	Noah-MP	CLM4.0	Bucket	Noah-MP	CLM4.0
Dryland cropland/pasture	− 1.08	*0.15*	0.28	− 0.26	*− 0.01*	0.04	− 9.40	*0.53*	0.70
Irrigated cropland/pasture	− 3.04	*0.26*	0.47	− 0.61	*− 0.01*	0.10	− 9.45	*0.53*	0.73
Mixed dry/irrigated crops	− 2.00	*0.25*	0.38	− 1.01	*0.07*	0.22	− 8.10	*0.79*	0.81
Mixed cropland/grassland	− 1.63	*0.14*	0.25	− 2.57	*0.44*	0.81	− 7.48	*0.73*	0.76
Mixed cropland/woodland	− 2.15	*0.21*	0.38	− 3.30	*0.52*	0.86	− 6.28	*0.73*	0.73
Grassland	− 2.39	*0.13*	0.35	− 5.12	*0.82*	1.19	− 5.90	*0.72*	0.74
Shrubland	− 2.52	*0.19*	0.42	− 5.93	*0.86*	1.34	− 5.60	*0.75*	0.86
Mixed shrubland/grassland	− 2.66	*0.27*	0.43	− 5.85	*0.89*	1.26	− 5.25	*0.63*	0.81
Savanna	− 2.52	*0.39*	0.47	− 6.16	*0.94*	1.19	− 4.26	*0.71*	0.82
Deciduous forest	− 2.53	*0.48*	0.54	− 6.00	*0.83*	1.13	− 4.47	*0.95*	1.06
Evergreen forest (needleleaf)	− 2.55	*0.56*	0.57	− 6.05	*0.89*	1.15	− 4.75	*1.12*	1.16
Water bodies	− 2.64	0.67	*0.56*	− 6.07	*0.84*	0.88	− 4.73	1.20	*1.12*
Herbaceous wetland	− 2.59	0.88	*0.69*	− 6.17	*0.83*	0.88	− 4.71	1.26	*1.23*

April, June, and August 2006 are included. The monthly value corresponding to the LSM with the lowest bias for each land use category is italicized

of the models' differences in handling of irrigation and soil moisture available for evapotranspiration (ET). CLM4.0 and Noah-MP both calculate soil moisture, and thus respond more realistically to abnormally dry conditions. The Bucket model may artificially increase ET and thus potential for moisture recycling and precipitation during dry conditions, since the evaporation rate with this LSM is restricted by the proportion of SWC to field capacity. SWC is prescribed in this LSM, leading to a high precipitation bias primarily in dry years. This is supported by the higher latent heat flux in the Bucket model output (e.g., Figs. 7 and 8). Also, handling of temperature and moisture in the boundary layer, which is sensitive to the representation of soil moisture and ET, partially determines whether the cumulus scheme is turned on and convective precipitation results. Thus, the amount of precipitation may vary substantially over small distances, potentially increasing the difference in precipitation between model output and observational data. Location of bias in precipitation output was highly variable between LSMs, as expected when averaging over monthly time scales in a region where convection is common (Fig. 5; Table 2). NARR precipitation was generally similar to PRISM observations (Fig. 5a, b).

When the same comparison of precipitation was made across the outer domain, results were again reasonably similar between the two sophisticated LSMs, which differed from the Bucket model. In CLM4.0 and Noah-MP (Fig. 6), too much precipitation was simulated in the eastern USA, while the Bucket model simulated too little precipitation there. Each LSM had relatively low precipitation bias in the western USA, though this is likely because total precipitation in that region is relatively small so the magnitude of bias will also be lower. All LSMs, particularly the sophisticated models, tended to produce too much precipitation over high-elevation regions in the West (Fig. 6). Magnitude of bias appeared relatively similar across the outer-inner domain boundary, again suggesting that increased spatial resolution in the inner domain may not meaningfully improve simulated precipitation.

3.3 Quantitative comparison to PRISM, ARM, and AmeriFlux observations

In order to quantitatively compare the WRF3.6-LSM results to PRISM data, the mean 2-m air temperature and monthly total precipitation for the inner domain were calculated for the three simulations. These domain-averaged values were compared to PRISM data averaged over the same domain. These comparisons yielded results consistent with those described previously for temperature and precipitation (Figs. 2 and 5; Tables 1 and 2). For April of the simulation years, CLM4.0 and Noah-MP were about 1 °C warmer and the Bucket model 2–3 °C cooler than PRISM (Table 1). In June and August, CLM4.0 and Noah-MP were on average 2–3 °C warmer than PRISM, while the Bucket model was 5–8 °C cooler than PRISM (Table 1).

The temperature bias was also computed for each land use type over the inner domain. Noah-MP performed the best overall with the smallest temperature bias (Table 3). Instances in which CLM4.0 had the smallest temperature bias either occurred in land use categories not dominant to the study region (e.g., wetlands and water bodies), were not consistent across months, and/or were not statistically significant

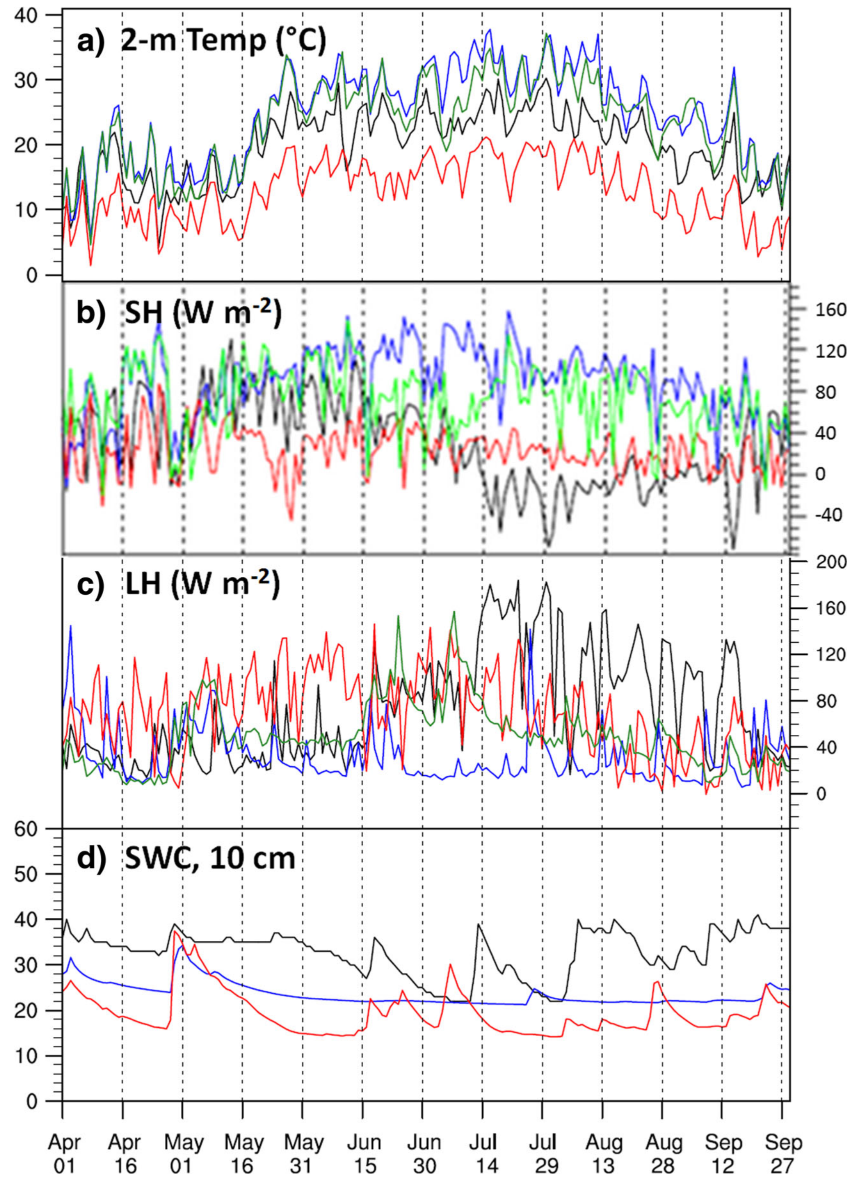

Fig. 7 Observations (black lines) and LSM output (CLM4.0: blue line; Noah-MP: green line; Bucket option: red line) for the Mead, Nebraska, AmeriFlux site for the months of April–September 2006. **a** Two-meter temperature. **b** Sensible heat flux. **c** Latent heat flux. **d** Ten-centimeter soil water content

(not shown). The Bucket model showed a persistent cool bias for each land use category. The magnitude of bias among the three LSMs increased as the warm season progressed (Table 1).

Some differences in precipitation bias are seen between simulations with the three LSMs, with Noah-MP results comparing more favorably with observations in many cases (Table 2). The Bucket option performed especially poorly during the 2012 drought, strongly overestimating total precipitation (Table 2). As mentioned prior, this was likely a consequence of unrealistically high ET, leading to excessive moisture recycling.

Point data from one ARM and one AmeriFlux site (Fig. 1) were also used for validation. Model output of temperature, sensible and latent heat, and SWC were compared to their site observations in 2006, a year with precipitation near the climatological average, at Mead, Nebraska (Fig. 7). While no LSM was clearly superior for these variables, several repeatable trends emerged. Noah-MP and CLM4.0 showed a warm bias relative to observations (Fig. 7a), while the Bucket option showed a strong cool bias. In observational data, sensible heating was relatively large early in the warm season and decreased during the middle and later portions of the warm season. Noah-MP and CLM4.0 showed substantial variability through the warm season but generally exhibited a high bias relative to observations, while sensible heating in the Bucket option was more consistent across the growing season (Fig. 7b), likely because of the aforementioned handling of ET. In observations from Mead, Nebraska, latent heating generally increases midway through the warm season but exhibits greater variability in the latter portion of the warm season (Fig. 7c). None of the LSMs produces this increased variability.

CLM4.0 is often too low in magnitude, and the Bucket option is again too steady through the warm season. SWC observations were generally higher than the values simulated by CLM4.0 and Noah-MP (Fig. 7d), though a similar variability emerges in response to rain events. The initial conditions for our simulations also may have had too low soil moisture, given the much higher observed values at the beginning of the warm season (Fig. 7d). Time series of SWC are not produced by the Bucket option.

In an effort to diagnose reasons for the observed temperature and precipitation biases, monthly mean ET and insolation were calculated for the inner domain (Table 4). The Bucket option generally produces the highest ET values, especially in 2012, an abnormally dry year. Insolation was almost always higher in CLM4.0 and Noah-MP than in Bucket (Table 4). In comparisons with AmeriFlux data from Mead, Nebraska, observed insolation was generally greater than that calculated by the Bucket option and less than that in CLM4.0 and Noah-MP (Table 4). Prior studies have noted a similar overestimate of insolation in WRF simulations (e.g., Markovic et al. 2008; Lu and Kueppers 2012). These results are consistent with theoretical expectations. While the Bucket model cannot adapt to changing soil moisture and ET, the more sophisticated LSMs may not be able to accurately represent the degree of irrigation over the study domain, resulting in higher ET in the Bucket option especially late in the warm season and lower ET in CLM4.0 and Noah-MP. Increased water vapor in the Bucket option could further translate to increased cloud cover and subsequently lower insolation values. These changes cause lower 2-m temperature, all else equal.

As a further validation of model results on a smaller temporal scale, mean monthly diurnal cycles of latent heat from the ARM site at Ashton, Kansas, were plotted for April, June, and August for the three study years (Fig. 8). All three LSMs simulate a diurnal cycle but differ strongly in magnitude. Diurnal variation of 2-m air temperature in the CLM4.0 and Noah-MP simulations was greater than observed, while that from the Bucket option was less. The Bucket option tended to produce the largest peak in latent heat, which was generally an overestimate compared to observations (Fig. 8). In agreement with Bowen ratio arguments, the Bucket option typically produced the lowest sensible heat flux for the diurnal cycle. This may help explain the negative temperature bias in simulations with the Bucket option, in conjunction with smaller insolation. As expected, the opposite was true for CLM4.0 and Noah-MP; extra sensible heating in those LSMs may partially explain their warm temperature biases. Simulations with the Bucket option generally performed the best in producing diurnal cycles of latent and sensible heat for 2006 (a near-normal precipitation year) at the Kansas ARM site, with inconclusive results for the abnormally wet and dry years. These results may indicate that the Bucket model describes the surface moisture process better in conditions near climatology, which seems reasonable since the water available for vegetation is fixed. CLM4.0 and Noah-MP outperform Bucket in years when precipitation differs substantially from the climatology.

4 Discussion and conclusions

The relative capabilities of three LSMs coupled with WRF3.6 to describe surface water and energy fluxes in the central USA were examined for the warm seasons of 2006 (near-normal precipitation), 2007 (anomalously wet), and 2012 (anomalously dry). Model output mean monthly temperature and total monthly precipitation were compared to PRISM data. Monthly mean ET and surface insolation were also computed

Table 4 Mean monthly evapotranspiration and surface insolation over the inner domain for April, June, and August of 2006, 2007, and 2012; comparison of received and simulated insolation values for the Mead, Nebraska, AmeriFlux site

	2006			2007			2012		
	April	June	August	April	June	August	April	June	August
Evapotranspiration (mm)									
CLM4.0	1.79	2.33	1.98	2.33	3.45	1.72	1.90	2.06	1.71
Noah-MP	1.45	2.42	2.14	1.94	3.54	2.04	1.64	2.36	1.82
Bucket	2.59	3.53	2.40	2.24	3.02	2.49	2.70	3.73	3.01
Surface insolation (W m^{-2})									
CLM4.0	265.9	343.1	282.6	257.2	320.8	294.1	272.9	341.3	287.4
Noah-MP	266.7	342.3	278.9	255.4	321.7	290.7	276.6	342.8	283.1
Bucket	249.5	326.3	246.6	248.6	313.4	269.8	257.3	329.4	286.5
Mead, Nebraska, surface insolation (W m^{-2})									
AmeriFlux	200.1	287.9	221.7	228.4	248.2	123.1	227.7	289.5	253.5
CLM4.0	247.1	331.0	266.8	242.2	325.9	269.3	252.2	343.8	276.7
Noah-MP	242.5	327.9	245.1	240.4	320.7	264.2	261.1	334.9	273.7
Bucket	206.5	297.7	187.3	224.3	306.3	223.3	213.5	295.4	228.5

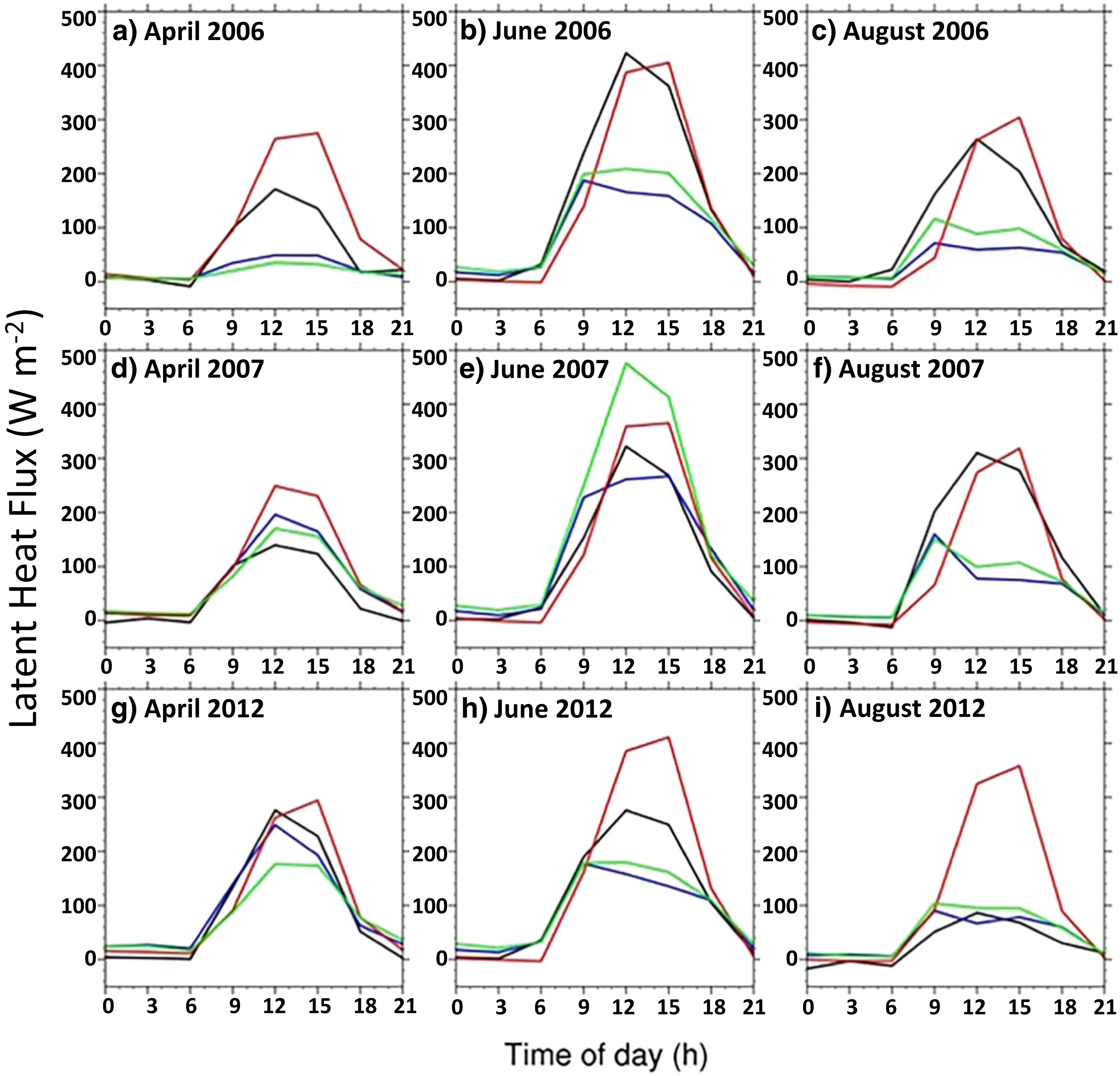

Fig. 8 Diurnal cycle of latent heat flux at the Ashton, Kansas, ARM site for April, June, and August 2006 (**a**–**c**), 2007 (**d**–**f**), and 2012 (**g**–**i**). Observed latent heat flux (black line), and output from CLM4.0 (blue line), Bucket model (red line) and Noah-MP (green line)

for the study area. Additionally, model outputs for temperature, LH, SH, and SWC were compared to observations.

A warm bias in 2-m air temperature was found in CLM4.0 and Noah-MP, and a larger cool bias was found using the Bucket option. These biases generally increased in magnitude as the warm season progressed, and were larger in the dry and normal-precipitation years. To diagnose reasons for these temperature biases, soil moisture, ET, surface insolation, and the surface energy partitioning between LH and SH were examined. Both CLM4.0 and Noah-MP had insolation of higher magnitude compared to the Bucket model. The two more sophisticated models also showed lower values of ET and LH but higher values of SH compared to the Bucket model. These differences partially explain the warm bias in CLM4.0 and Noah-MP. In addition, lower insolation in the Bucket model helps explain why it often had a large cool bias. SWC was generally underestimated in CLM4.0 and Noah-MP compared to observations. This lower SWC appeared to be contributing to the increased SH and therefore warmer 2-m temperatures. Lower SWC in the CLM4.0 and Noah-MP also appeared to be contributing to a smaller cloud fraction in those simulations, leading to larger surface insolation and warmer temperature values. Increased LH and thus boundary layer moisture in the Bucket option appeared to contribute to a larger cloud fraction, further reducing 2-m temperature. Further work should examine reasons for the high temperature bias over this region in the warm season, and reasons for why the magnitude of this bias tends to be lower in wet years.

The smaller temperature biases in CLM4.0 and Noah-MP compared to the Bucket model are likely attributable to a better handling of soil moisture by the more sophisticated models. Both CLM4.0 and Noah-MP have multiple soil layers at which soil moisture is calculated, and better capabilities to handle hydrologic processes in the rooting zone. An accurate depiction of soil moisture is critical for the proper handling of energy partitioning between LH and SH. All three LSMs adequately simulated the diurnal variability of temperature and LH/SH but with differences in magnitude.

Precipitation was simulated less accurately than temperature by all three LSMs, an expected result because of the large temporal and spatial variability of precipitation events. Nonetheless, these LSMs produced similar patterns of wet and dry biases, again with the largest differences between CLM4.0/Noah-MP and the Bucket model. These differences between LSMs were largest in 2012, a regional drought year, as were their biases compared to observations. The biases from these LSMs were often not consistent across the warm season or during the same month in different years. A topic of future work will be to investigate in much more detail how precipitation characteristics change as a function of the land surface. It would also be interesting to test the sensitivity of simulated precipitation in this region to the microphysics parameterization used.

Variations in output from high-resolution regional models can be caused by many factors, including remote forcing, microphysics, and convective parameterization scheme, all of which were held constant in these simulations. The model output is also sensitive to how each LSM handles soil and vegetation processes. CLM4.0 and Noah-MP are both more complex in allowing for sub-grid calculations and attempting to handle the relevant biophysics. They may not, however, adequately represent human influences such as irrigation, especially during drought years, or rapidly changing land use in some areas. Future studies examining the effects of land use change and irrigation could help close this gap between model simulations and observations. Studies with the dynamic vegetation option turned on would also be insightful and may help determine what improvements would be helpful to improve model ability to describe land surface processes in various situations.

It is important to consider the goals and resources of a study prior to selecting a LSM, as each has its advantages and disadvantages. For example, CLM4.0 is better equipped to handle differing vegetation types and thus may be best for studies directly examining this topic. This LSM also contains additional output variables, such as more extensive and deeper soil moisture and temperature, which may be useful for answering some research questions. However, CLM4.0 is also much more computationally intensive than Noah-MP without providing demonstrably better results, at least for the domain examined in this study. Thus, it may not be feasible or necessary to use CLM4.0 if the effects of vegetation and deep soil information are not the primary focus of research, or if the additional output variables are not needed. With this in mind, both CLM4.0 and Noah-MP are scientifically viable options for examining the effects of land-atmosphere interactions on climate for the central USA in the warm season, while the limitations of the Bucket option make it less suitable for such a study in this domain.

Acknowledgements We acknowledge high-performance computing support from Yellowstone (ark:/85065/d7wd3xhc) provided by the National Center for Atmospheric Research's (NCAR's) Computational and Information Systems Laboratory (CISL), sponsored by the National Science Foundation. We also acknowledge the Holland Computing Center at the University of Nebraska, which receives support from the Nebraska Research Initiative, for the use of computing resources. The authors thank three anonymous reviewers and Cindy Hays for substantial contributions to the project.

Funding information Support for this research was provided by the National Science Foundation (Grant No. AGS-1355916).

References

Anthes RA (1984) Enhancement of convective precipitation by mesoscale variations in vegetative covering in semiarid regions. J Clim Appl Meteorol 23:541–554

Baldocchi D, Falge E, Gu L, Olson R, Hollinger D, Running S, Anthoni P, Bernhofer C, Davis K, Evans R (2001) FLUXNET: a new tool to study the temporal and spatial variability of ecosystem-scale carbon dioxide, water vapor, and energy flux densities. Bull Am Meteorol Soc 82:2415–2434

Bowen IS (1926) The ratio of heat losses by conduction and by evaporation from any water surface. Phys Rev 27:779–787

Budyko MI (1961) The heat balance of the Earth's surface. National Weather Service, U.S. Department of Commerce, Washington, D.C.

Bukovsky MS, Karoly DJ (2009) Precipitation simulations using WRF as a nested regional climate model. J Appl Meteorol Climatol 48:2152–2159

Charney J, Stone PH, Quirk WJ (1975) Drought in the Sahara: a biogeophysical feedback mechanism. Science 187:434–435

Chen F, Liu C, Dudhia J, Chen M (2014) A sensitivity study of high-resolution regional climate simulations to three land surface models over the western United States. J Geophys Res Atmos 119. https://doi.org/10.1002/2014JD021827

Copeland JH, Pielke RA, Kittel TGF (1996) Potential climatic impacts of vegetation change: a regional modeling study. J Geophys Res Atmos 101:7409–7418

Daly C, Halbleib M, Smith JI, Gibson WP, Doggett MK, Taylor GH, Curtis J, Pasteris PP (2008) Physiographically sensitive mapping of climatological temperature and precipitation across the conterminous United States. Int J Climatol 28:2031–2064

Dudhia J (1989) Numerical study of convection observed during the Winter Monsoon Experiment using a mesoscale two–dimensional model. J Atmos Sci 46:3077–3107

Dudhia J (1996) A multi-layer soil temperature model for MM5. Preprints, The 6th PSU/NCAR Mesoscale Model Users Workshop, 22–24 July 1996, Boulder, CO, 49–50
Giambelluca TW, Hölscher D, Bastos TX, Frazão RR, Nullet MA, Ziegler AD (1997) Observations of albedo and radiation balance over postforest land surfaces in the eastern Amazon Basin. J Clim 10:919–928
Hack JJ, Caron JM, Danabasoglu G, Oleson KW, Bitz C, Truesdale JE (2006) CCSM-CAM3 climate simulation sensitivity to changes in horizontal resolution. J Clim 19:2267–2289
Hong S-Y, Dudhia J, Chen S-H (2004) A revised approach to ice microphysical processes for the bulk parameterization of clouds and precipitation. Mon Weather Rev 132:103–120
Huang D, Liu Y (2015) A novel approach for introducing cloud spatial structure into cloud radiative transfer parameterizations. Environ Res Lett 9:124022
Huber DB, Mechem DB, Brunsell NA (2014) The effects of Great Plains irrigation on the surface energy balance, regional circulation, and precipitation. Climate 2:103–128
Jin J, Miller NL, Schlegel N (2010) Sensitivity study of four land surface schemes in the WRF model. Adv Meteorol 2010:11
Kain JS (2004) The Kain-Fritsch convective parameterization: an update. J Appl Meteorol 43:170–181
Kain JS, Fritsch JM (1990) A one-dimensional entraining/detraining plume model and its application in convective parameterization. J Atmos Sci 47:2784–2802
Lawrence DM, Oleson KW, Flanner MG, Thornton PE, Swenson SC, Lawrence PJ, Zeng X, Yang Z, Levis S, Sakaguchi K, Bonan GB, Slater AG (2011) Parameterization improvements and functional and structural advances in version 4 of the Community Land Model. J Adv Model Earth Syst 3:27
Li W, Guo W, Xue Y, Fu C, Qiu B (2016) Sensitivity of a regional climate model to land surface parameterization schemes for East Asian summer monsoon simulation. Clim Dyn 47:2293–2308
Liu C et al (2016) Continental-scale convection-permitting modeling of the current and future climate of North America. Clim Dyn 49:71–95
Lu Y, Kueppers LM (2012) Surface energy partitioning over four dominant vegetation types across the United States in a coupled regional climate model (Weather Research and Forecasting Model 3 Community Land Model 3.5). J Geophys Res Atmos 117:D06111
Lu Y, Jin J, Kueppers LM (2015) Crop growth and irrigation interact to influence surface fluxes in a regional climate-cropland model (WRF3.3-CLM4crop). Clim Dyn 45:3347–3363
Luo YQ et al (2012) A framework for benchmarking land models. Biogeosciences 9:3857–3874
Lyons TJ, Xinmei H, Schwerdtfeger P, Hacker JM, Foster IJ, Smith RCG (1993) Land–atmosphere interaction in a semiarid region: the bunny fence experiment. Bull Am Meteorol Soc 74:1327–1334
Mahmood R, Foster SA, Keeling T, Hubbard KG, Carlson C, Leeper R (2006) Impacts of irrigation on 20th century temperature in the northern Great Plains. Glob Planet Chang 54:1–18
Mahmood R, Hubbard KG, Leeper RD, Foster SA (2008) Increase in near-surface atmospheric moisture content due to land use changes: evidence from the observed dewpoint temperature data. Mon Weather Rev 136:1554–1561
Mahmood R et al (2014) Land cover changes and their biogeophysical effects on climate. Int J Climatol 34:929–953
Manabe S (1969) Climate and the ocean circulation—part 1: the atmospheric circulation and the hydrology of the earth's surface. Mon Weather Rev 97:739–774
Markovic M, Jones CG, Vaillancourt PA, Paquin D, Winger K, Paquin-Ricard D (2008) An evaluation of the surface radiation budget over North America for a suite of regional climate models against surface station observations. Clim Dyn 31:779–794
Mesinger F et al (2006) North American regional reanalysis. Bull Am Meteorol Soc 87:343–360
Mlawer E, Steven J, Taubman J, Brown PD, Iacono MJ, Clough SA (1997) Radiative transfer for inhomogeneous atmospheres: RRTM, a validated correlated–k model for the longwave. J Geophys Res Atmos 102:16663–16682
Mo K, Schemm J (2008) Droughts and persistent wet spells over the United States and Mexico. J Clim 21:980–994
Nair US, Wu Y, Kala J, Lyons TJ, Pielke RA Sr, Hacker JM (2011) The role of land use change on the development and evolution of the west coast trough, convective clouds, and precipitation in southwest Australia. J Geophys Res Atmos 116:D07103
Niu G et al (2011) The community Noah land surface model with multiparameterization options (Noah-MP): 1. Model description and evaluation with local-scale measurements. J Geophys Res Atmos 116:D12109
Oglesby RJ, Erickson DJ (1989) Soil moisture and the persistence of North American drought. J Clim 2:1362–1380
Oglesby RJ, Marshall S, Roads JO, Robertson FR (2001) Diagnosing warm season precipitation over the GCIP region from a GCM and reanalysis. J Geophys Res Atmos 106:3357–3369
Oglesby RJ, Marshall S, Erickson DJ III, Roads JO, Robertson FR (2002) Thresholds in atmosphere-soil moisture interactions: results from climate model studies. J Geophys Res Atmos 107:ACL15–1–ACL15–15
Oleson KW, Lawrence DM, Bonan GB, Flanner MG, Kluzek E, Lawrence PJ, Levis S, Swenson SC, Thornton PE (2010) Technical description of version 4.0 of the Community Land Model (CLM). NCAR, 266 pp. [Available online at http://www.cesm.ucar.edu/models/ccsm4.0/clm/CLM4_Tech_Note.pdf]
Otterman J, Chou M-D, Arking A (1984) Effects of nontropical forest cover on climate. J Clim Appl Meteorol 23:762–767
Pielke RA, Dalu GA, Snook JS, Lee TJ, Kittel TGF (1991) Nonlinear influence of mesoscale land use on weather and climate. J Clim 4: 1053–1069
Pitman AJ (2003) The evolution of, and revolution in, land surface schemes designed for climate models. Int J Climatol 23:479–510
Prein AF et al (2015) A review on regional convection-permitting climate modeling: demonstrations, prospects, and challenges. Rev Geophys 53:323–361
PRISM Climate Group (2015) Oregon State University, http://prism.oregonstate.edu. Accessed 20 Jan 2017
Rojas M (2006) Multiply nested regional climate simulation for southern South America: sensitivity to model resolution. Mon Weather Rev 134:2208–2223
Skamarock W, Klemp J, Dudhia J, Gill D, Barker D, Wang W, Powers J (2008) A description of the advanced research WRF version 3. NCAR Tech. Note NCAR/TN-4751STR, 113 pp
Subin ZM, Riley WJ, Jin J, Christianson DS, Torn MS, Kueppers LM (2011) Ecosystem feedbacks to climate change in California: development, testing, and analysis using a coupled regional atmosphere and land-surface model (WRF3-CLM3.5). Earth Interact 15:1–38
Weaver CP (2004) Coupling between large-scale atmospheric processes and mesoscale land–atmosphere interactions in the U.S. Southern Great Plains during summer. Part II: mean impacts of the mesoscale. J Hydrometeorol 5:1247–1258
Wei J, Dirmeyer PA, Guo Z, Zhang L, Misra V (2010) How much do different land models matter for climate simulation? Part I: climatology and variability. J Clim 23:3120–3134
Woodhouse CA, Overpeck JT (1998) 2000 years of drought variability in the central United States. Bull Amer Meteorol Soc 79:2693–2714